

Efficient reflectivity modelling for full wavefield FWI

Tony Martin^{1*}, Yang Yang², Norman Daniel Whitmore², Nizar Chemingui², Tiago Alcantara² and Eric Frugier² describe an efficient modelling of reflectivity to drive full wavefield full waveform inversion. Reformulating the variable density acoustic wave-equation in terms of vector-reflectivity, represents a step towards full automation, and enables a greater diversity of applications.

Challenges of reflection-inclusive FWI

As full waveform inversion (FWI) becomes more commonplace, the demand for application diversity grows. Conventional inversion approaches may struggle in challenging geological settings or where the data diversity is poor. In these environments, FWI may create accurate high-resolution models, as it directly uses the seismic data, not measures from it.

Historical FWI applications have focused on using transmission energy, sometimes referred to as refraction FWI. However, most conventional acquisition geometries have limitations in their design, and consequentially the FWI model updates using only transmission have a limited impact with depth. Simultaneous use of reflections and transmission, free of any need to manipulate the seismic data, would enable a cost-effective acceleration of deeper FWI updates, replete with resolution in all dimensions.

There are challenges with incorporating reflections in FWI, primarily but not exclusively within the modelling engine. For example, how do we model the reflections that are necessary for a full wavefield FWI? They are present in the acquired seismic data, so their accurate modelling is needed to avoid building bad models for deeper data. Seismic modelling may overcome this with hard boundaries in the velocity model or with an accurate density model, but only if we have access to them.

Recorded seismic data does not directly measure density, and in underexplored regions density models may be difficult to access or generate. In these areas highly evolved velocity models probably do not exist. So, how are the reflections generated, especially if boundary contrasts are significant? There is an added complication. Relying on boundaries in either velocity or density may cause a decoupling of the modelled reflections from the true sub-surface – do we know whether the real reflectivity is a function of one or other? This assumption may lead to parameter leakage in the inversion, resulting in an inaccurate model.

Another critical component of reflection-inclusive FWI is to exclude the high-wavenumber (perturbation) data when updating the long-wavelengths (background) of the velocity model. Failure to build the correct background model may lead to inversion results that resemble seismic images. There are different strategies to separate the low- from the high-wavenumber

components of the velocity updates. The most common industry approach is using the Born approximation and perturbation theory. This involves the cascade of two different solutions to the acoustic wave-equation (Mora, 1989), decomposing the seismic wavefields into background and perturbation components. By using a combination of two approaches, this approximate solution increases the computational costs.

Reformulation enables accurate modelling using the measured data

Reformulating the variable density acoustic wave-equation used for modelling in terms of parameters that are directly measurable from the recorded seismic data, e.g. velocities and reflectivity, avoids the cumbersome and potentially inaccurate task of indirectly estimating density from the data, or from sparse well measures. Berkout (1981) developed a one-way wave-equation method for modelling with velocity and reflectivity. Subsequent work on joint migration-inversion (Berkhout, 2012), and demonstrated in Verschuur et al. (2016) addressed the one-way limitations for modelling with velocity and reflectivity, but requires FWI to accommodate the transmission wave component necessary for full wavefield model building. We demonstrate an approach that utilizes the benefits of the full wavefield, within one FWI algorithm, using one gradient computation, to generate a model.

The variable density acoustic wave-equation is defined by a temporally and spatially varying pressure wavefield, velocity, density and a source component. Acoustic impedance is a function of spatially varying density and velocity, and enables a reformulation of the density wave-equation to one defined by reflectivity, where vector-reflectivity is defined as the normalized rate of acoustic impedance change in each vector direction (Sheriff and Geldart, 1995). Using this reformulation, scattering is primarily produced by the reflectivity term. No approximations are made, and only one wave-equation needs to be solved, comparing favourably with the two required by Born modelling (Mora, 1989). This approach enables a new and efficient modelling engine for an FWI workflow for the full wavefield, using both transmission and reflections.

In conjunction with this new modelling engine, and to complete the optimized FWI workflow, the separation of low- and

¹ PGS UK | ² PGS USA

* Corresponding author, E-mail: tony.martin@pgs.com

DOI: 10.3997/1365-2397.fb2021019

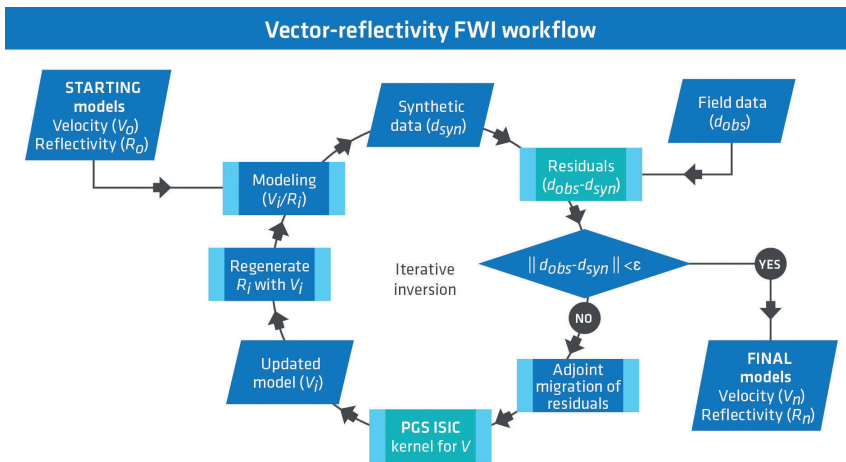


Figure 1 A schematic of the full wavefield FWI approach using vector-reflectivity.

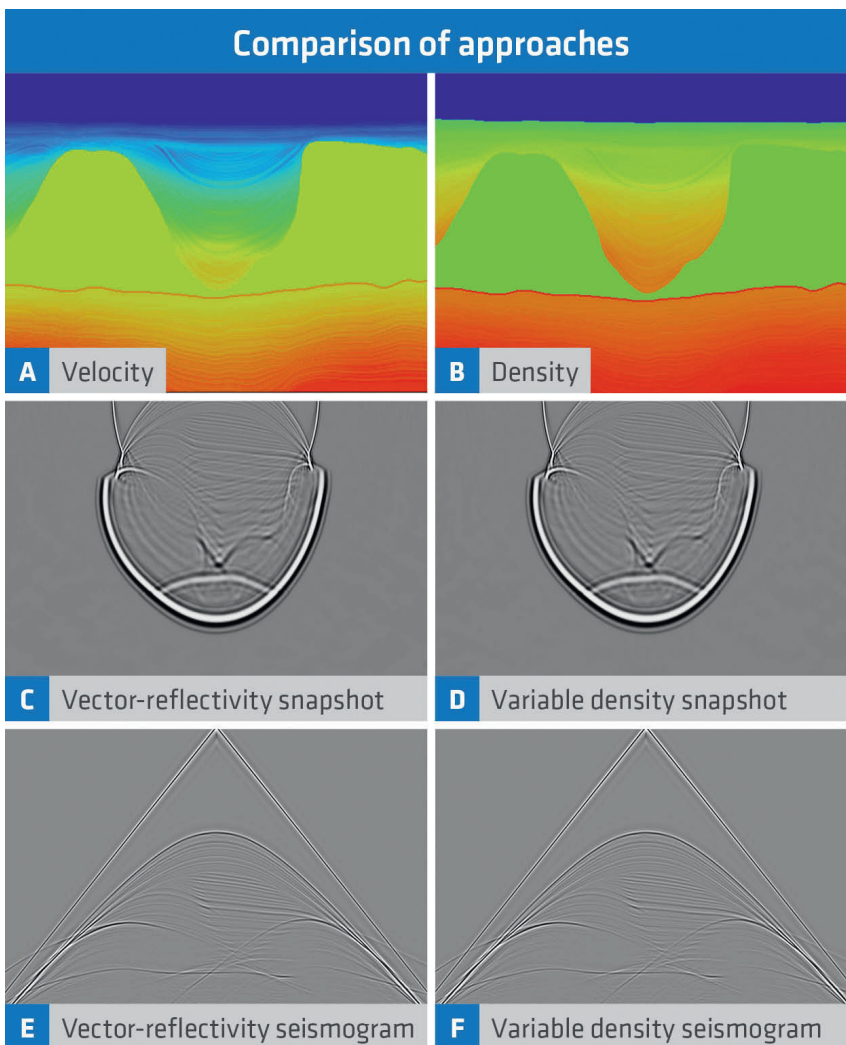


Figure 2 A and B – models used for the vector-reflectivity and density modelling comparison. C and D – a wavefield snapshot using the two approaches. E and F – surface seismograms using the two approaches. Note how both C and D, and E and F are almost identical, validating the vector-reflectivity reformulation.

high-wavenumber components in the gradient is determined by the method outlined by Ramos-Martinez et al. (2016), which uses a variant on an inverse scattering imaging condition. The reflectivity term is derived directly from seismic imaging and the velocity model comes from either tomography or FWI. A schematic of the workflow is outlined in Figure 1. The inversion scheme jointly updates both the velocity and the reflectivity terms in each pass; the regeneration of the reflectivity term, based on the updated velocity model, is needed to maintain accurate reflection

modelling for each successive iteration, which continues until the objective function criterion is reached.

The advantages of using a velocity and vector-reflectivity wave-equation for modelling in FWI are:

- No need to construct a density model or have an accurate velocity model with hard boundaries
- It only uses one wave-equation, not two as used in conventional Born modelling and perturbation theory approaches

- It is equivalent to the variable density wave-equation and no approximations are made
- It accelerates the turnaround of full wavefield FWI model building
- It enables a step towards automation and joint inversion for velocity and impedance over the entire record

We illustrate the use of a velocity and vector-reflectivity driven full wavefield FWI, showing modelling equivalence to the variable density wave-equation in a synthetic study, and deep reflection updates using a field data example.

Example one — validating the vector-reflectivity acoustic wave-equation

To validate the reformulation, we use the velocity and density models shown in Figures 2A and 2B, and compare the results of modelled data using both the variable density and the vector-reflectivity acoustic wave-equations. For this example directional changes in impedance were used to derive the vector-reflectivity model. In day-to-day practice, the seismic image is used to determine the reflectivity (Whitmore et al., 2020).

The confirmation test compares snapshots of the wavefield propagation and their resulting shot profile seismograms. The wavefield snapshots (Figure 2C and 2D) for the two approaches are almost identical, differences are very difficult to determine. The surface seismograms (Figures 2E and 2F) display a comparable likeness, demonstrating an equivalence of the two approaches. Importantly, this result shows how accurate reflection modelling can be achieved without knowledge of the density profile in the area. This is significant, as it is easier to approximate the reflectivity from the seismic image than to derive an accurate density model, especially in areas with poor well control.

Example Two — Application to solve deep data velocity model building using full wavefield FWI

The benefits of the new modelling code are illustrated on field seismic data from the Orphan basin, located in the north of the Grand Banks, North East of St John's, Canada. Analysis of the data suggests Jurassic source rocks, with reservoirs in Tertiary, Cretaceous and upper Jurassic sequences. There are a small number of wells in the area, with some showing an amplitude versus

offset response indicative of fluid-filled reservoirs in Cretaceous and upper Jurassic formations. The wells also confirm two source rock sequences (Alcantara et al., 2020).

The multi-layered source and reservoir formations occur over an extended data range, with the upper Cretaceous occurring at approximately 4 km depth. Figure 3 illustrates the location of the Tablelands data used in the case study.

The newly acquired data, shot in 2019 using 16 multisensor streamers, each 100 m apart and 8000 m long, used a comprehensive and tailored processing sequence including a full wavefield FWI to ensure accurate imaging for all target sequences, and to maintain data integrity for a least-squares migration of the data. This under-explored area had no accurate legacy 3D velocity models, well density was sparse, and the acquisition had limited offsets.

FWI implementation

In practice, FWI was run as a multi-stage process, building up from 4 Hz to 25 Hz, and building out in offset to 8000 m. The input velocity model for FWI was derived using wavelet shift tomography (Sherwood et al., 2008). Initial FWI sensitivity kernels using only transmission energy showed a 4 km depth of penetration. This represents an update limited to the Base Tertiary sequence, and is the consequence of the water depth (2 km), the sub-surface gradient and the acquisition geometry.

The full wavefield updates used in the production phase of the project produced a structurally conformable model in the deeper data, despite the limitations of offset coverage and illumination. A lack of density control, or deep boundaries in the evolving velocity model created some challenges with the reflectivity modelling, and consequently curtailed updates from the deeper data.

Amplitude misfits and cross-correlation statistics were used to evaluate the model as it evolved. After each scale additional quality control (QC) was performed in both data and image domains ensuring both model resolution and the migrated image improved. QC included comparisons of modelled and recorded shots and receivers, updated difference, and migrated common image point gathers and stacks before and after each pass.

The model captured the small-scale geological features in the Tertiary section, which are clearly visible in the vertical sections shown in Figure 4. The velocity model and update difference show

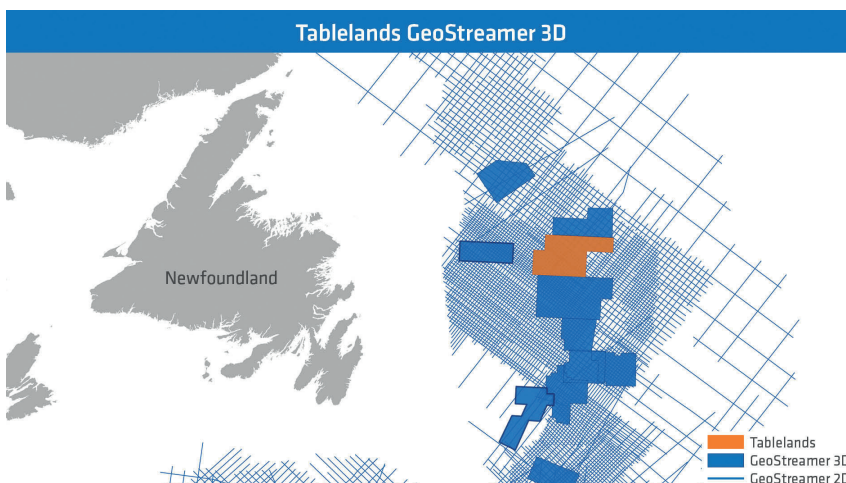


Figure 3 Map outlining the location of the Tablelands data set.

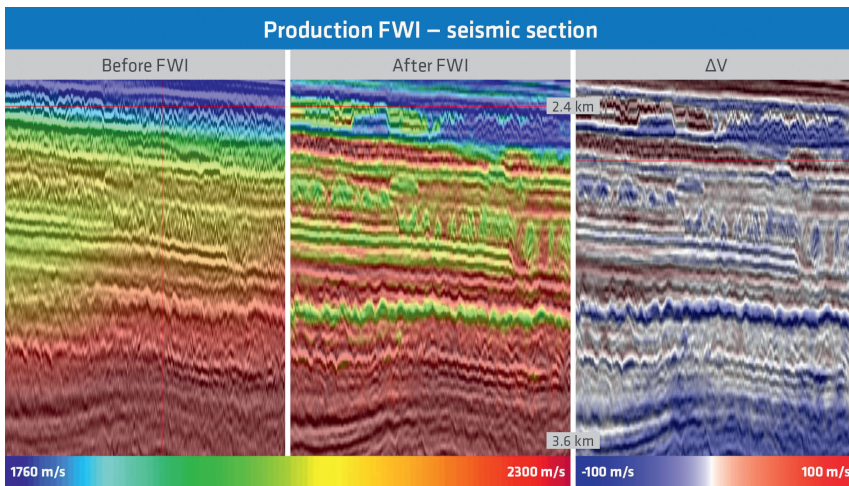


Figure 4 Single vertical section showing the input (left) and output (centre) from the 25 Hz FWI work. The difference (right) shows how FWI has accurately delineated the localized fast and slow intervals, and introduced a level of both vertical and spatial resolution not achievable using a conventional approach.

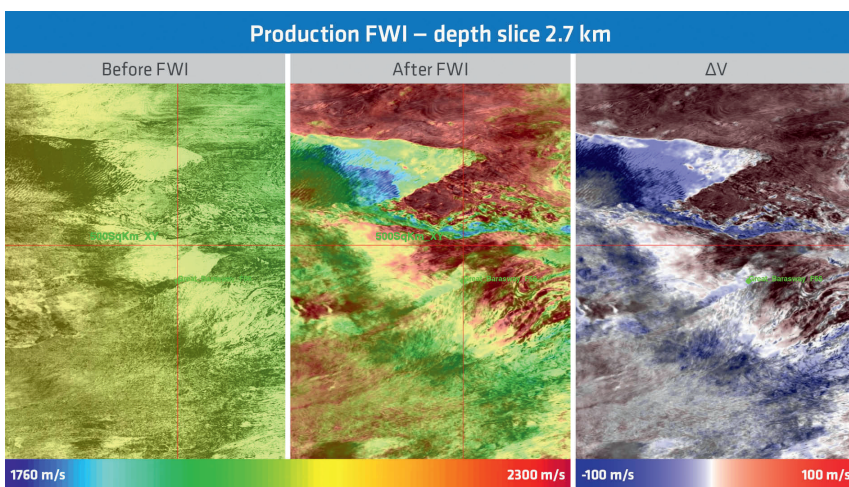


Figure 5 Single depth slice showing the input (left) and output (centre) from the 25 Hz FWI work. The difference (right) shows how FWI has accurately delineated the localized fast and slow intervals, conforming to the local structure seen within the data.

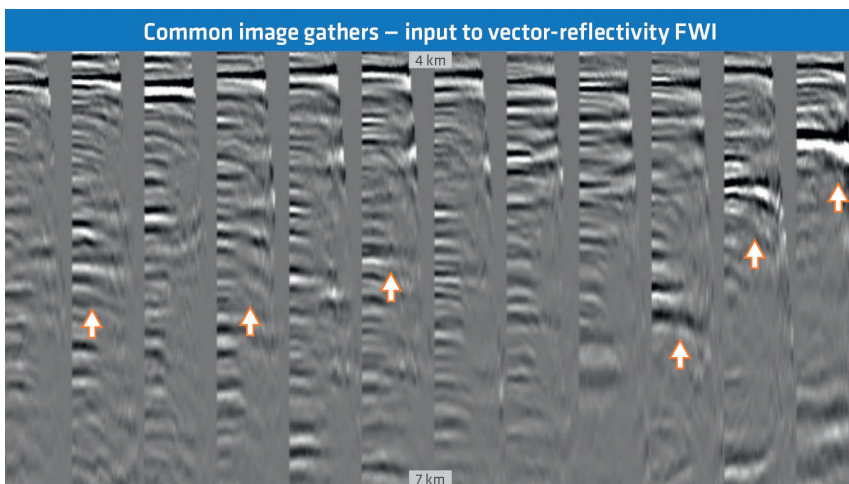


Figure 6 Common Image Gathers (CIGs) migrated with the production FWI model. Orange arrows indicate areas where the events are under-corrected. These localized events exist beyond the penetration of the FWI model.

isolated events and local variations in sequences, with layering and boundaries conforming to the reflectivity. Improvements to the spatial resolution, along with the delineation of the Tertiary channel are evident in the depth slices shown in Figure 5. Using reflection energy, several velocity inversions were modelled, particularly in the shallow overburden, and the updated velocity model closely followed the regional structural trend in the deeper Jurassic section.

The model was then used for an additional pass of vector-reflectivity FWI, to update the deeper Cretaceous and Jurassic target

sequences. A near angle migrated stack, using the production FWI model, was used for the vector-reflectivity FWI case study. The short-spread was selected to minimize any traveltimes errors for the reflectivity modelling. Figure 6 shows the migrated common image point gathers (CIGs) using the production FWI model. The orange arrows highlight that the majority of events are under-corrected in this area, and need the model to ‘slow-down’ below 4 km depth.

In Figure 7, the update difference from the vector-reflectivity FWI case study is co-rendered on the seismic data, and shows

a systematic slow-down. The difference shows excellent spatial resolution, correlating with the sub-surface structure; updates are accurately constrained within isolated faulted blocks and layered sequences. The inversion produces results to a depth of 7.5 km, at which point reflectivity within the seismic data gives way to a lengthy opaque section.

The updated model from the vector-reflectivity FWI is shown in Figure 8. The depth slice is at approximately 4.5 km depth, and the blue arrow indicates the region of the model shown as a difference in Figure 7, where the updated slow-down is clearly visible. The improvement in resolution is clear. The CIGs resulting from the migration using the new approach's model show a clear improvement in gather flatness (Figure 9).

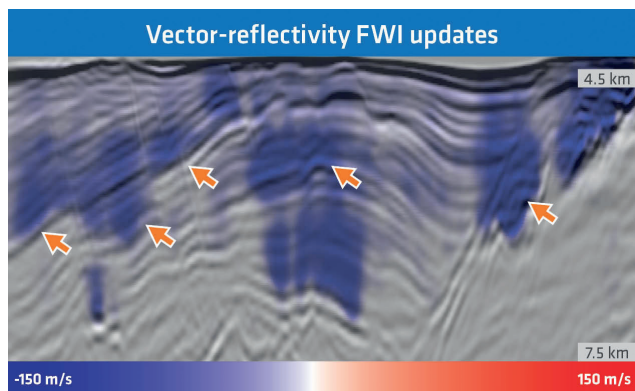


Figure 7 Vector-reflectivity FWI update for a single vertical section. Orange arrows indicate the structural conformity of the update, constrained by both faulting and sequence boundaries.

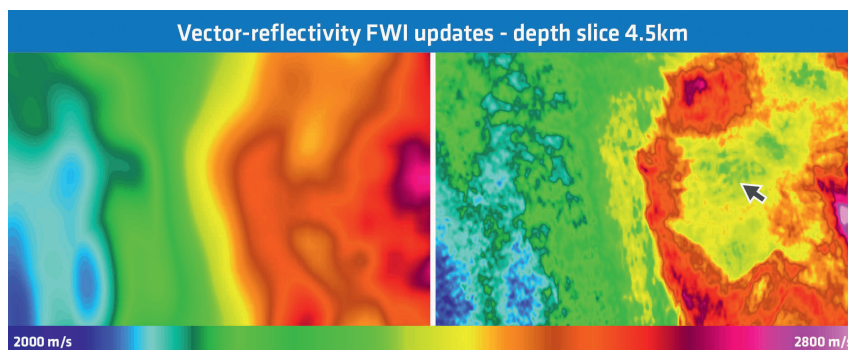


Figure 8 Depth slice of the input (left) and output (right) models for the vector-reflectivity FWI. The blue arrow highlights the area where a slow-down was required for the input model and data. The output FWI model enhanced spatial resolution at depths of greater than 4.5 km.

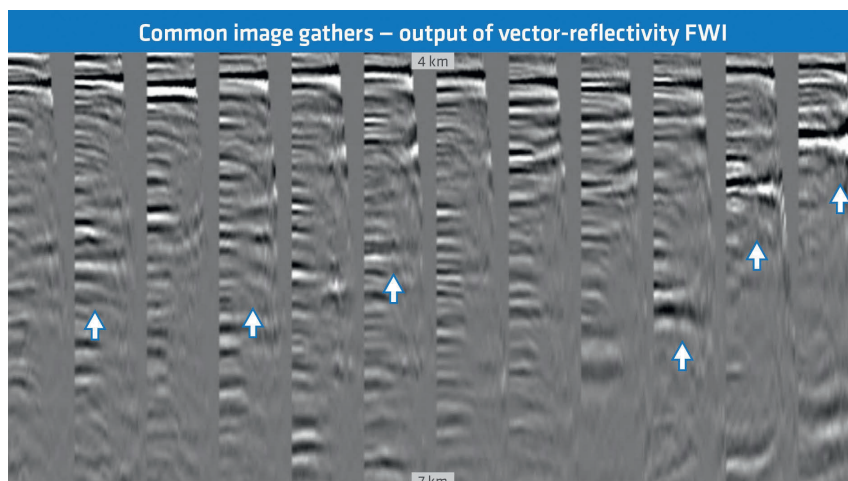


Figure 9 Common Image Gathers (CIGs) migrated with the vector-reflectivity FWI model. Blue arrows indicate events that were previously under-corrected, but are now flatter to greater offset.

Blue arrows highlight locations where the events across offsets are considerably flatter than those highlighted by orange arrows in Figure 6.

Discussion

Reflection-inclusive FWI is necessary for accurate velocity model building where transmission-driven FWI has limited penetration, and conventional methods fail. There are challenges including reflections in FWI. We have outlined, with examples, an efficient way to incorporate their modelling for a full wavefield FWI. By defining the variable density acoustic wave-equation in terms of velocity and reflectivity, parameters directly measurable from the data, a seismic image can be used to accommodate the modelling of reflections, enabling a full wavefield FWI.

A number of industry implementations of FWI invert for velocity and pragmatically associate a reflectivity product with the resulting velocity model (e.g. Qin et al., 2015; Kalinicheva et al., 2020). Some of these approaches assume that reflectivity is primarily a function of velocity, and that the creation of the reflectivity data may be done using a simplistic estimate of density along with the derivative of the velocity, sometimes determined vertically; whilst others allow high-wavenumber perturbation leakage in the imaging condition of FWI.

The method presented in this paper uses a reflectivity image taken directly from the seismic data as an auxiliary data set and is coupled with an innovative inverse scattering imaging condition which, when used together, significantly simplifies the use of reflections in a reflection-inclusive FWI. The implementation updates both the velocity and reflectivity, maintaining accurate

reflection modelling and representing a step towards a fully automated inversion solution.

Additional model constraints, using a variable weighted L^1 norm of the total variation of the model, are also added to the objective function (Qiu et al., 2016; Martin et al., 2017). This is particularly useful for pursuing a sparse representation of the model in the presence of large contrasts, this approach enables a multi-dimensional model constraint on the objective function, preserving the resolution of the model while removing spurious noise during the inversion.

Using a full wavefield FWI allows a greater diversity of applications. The implementation demonstrated here is a cost-effective FWI workflow, able to produce models beyond the limitations of transmission energy, where density models are difficult to determine and velocity models are under-developed. It requires no data manipulation or manual intervention, and enables accurate model building using FWI over the full record, resulting in improved imaging and consequently more accurate seismic data for interpretation and reservoir characterization.

Summary and conclusions

Using reflections in FWI can be challenging. However, their generation is necessary for an accurate full-record inversion. To achieve this the modelling engine needs a velocity model with hard boundaries, or an accurate density model. In underexplored areas, neither of these are frequently available. Therefore, model building with the benefits of FWI can be limited, and processing sequences need to resort to inversion schemes where measures are extracted from the data, rather than using the data itself. In environments where large velocity contrasts exist, or data diversity is poor, these methods may also fail.

Converting the variable density acoustic wave-equation to a vector-reflectivity one, allows accurate modelling of reflections for FWI. The seismic image is used as an auxiliary data set, supporting modelling of reflections for a full record full wavefield FWI. In our first example we demonstrated modelling equivalence with the variable density acoustic wave-equation, and in the second case study the benefits of full record velocity model building using this new approach. The method updates both the velocity model and reflectivity volume, maintaining precision for the modelling of reflections in FWI, and resulting in accurate and high-resolution model building over the full record. This is essential for quantitative interpretation as an accurate velocity model reduces uncertainty in spatial positioning, whilst improving the focusing of seismic energy.

Acknowledgements

The author's wish to thank PGS for permission to publish the paper. We would also like to thank our joint venture partners TGS, and Oil and Gas Newfoundland and Labrador.

References

- Alcantara, T., Frugier, E. and Virlovet, B. [2020] High-resolution velocity model building and least-squares imaging offshore Canada: a deep-water Orphan Basin example, *90th Annual International Meeting, SEG*, Expanded Abstracts.
- Berkout, A.J. [1981] Wave field extrapolation techniques in seismic migration, a tutorial, *Geophysics*, **46**(12), 1638-1656.
- Berkhout, A.J. [2012] Combining full wavefield migration and full waveform inversion, a glance into the future of seismic imaging: *Geophysics*, **77**, S43-S50
- Kalinicheva, T., Warner, M. and Mancini, F. [2020] Full-Bandwidth FWI, *82nd EAGE Conference & Exhibition*, Extended Abstracts.
- Martin, T., Pendred, G., Vermeulen, J., Bell, M. and Mellar, P. [2017] A robust FWI method for model updating in high contrast bodies. *79th EAGE Conference and Exhibition*, Extended Abstracts, Th B1 09.
- Mora, P. [1989] Inversion = migration + tomography, *Geophysics*, **54**(12), 1575-1586.
- Qin, B., Allemand, T. and Lambaré G. [2015] Full waveform inversion using preserved amplitude reverse time migration, *85th Annual International Meeting, SEG*, Expanded Abstracts, 1252-1257.
- Qiu, L., Zou, K., Valenciano, A.A. and Chemingui, N. [2016] Full waveform inversion with steerable variation regularization, *86th Annual International Meeting, SEG*, Expanded Abstracts.
- Ramos-Martinez, J., Crawley, S., Zou, K., Valenciano, A.A., Qiu L. and Chemingui N. [2016] A robust gradient for long wavelength FWI updates, *78th EAGE Conference & Exhibition*, Extended Abstracts.
- Sheriff, R.E. and Geldart, L.P. [1995] *Exploration Seismology*, Cambridge University Press, 2nd Edition.
- Sherwood, J.W.C., Sherwood, K., Tieman, H. and Schleicher, K. [2008] 3D beam prestack depth migration with examples from around the world. *78th Annual International Meeting, SEG*, Expanded Abstracts, 438-442.
- Verschuur, D.J., Staal, X.R. and Berkhout, A.J. [2016] Joint migration inversion: Simultaneous determination of velocity fields and depth images using all orders of scattering. *The Leading Edge*, **35**, 1037-1046.
- Whitmore, N.D., Ramos-Martinez, J., Yang, Y. and Valenciano, A.A. [2020] Full wavefield modeling with vector-reflectivity, *82nd EAGE Conference & Exhibition*, Extended Abstracts.